Available online at www.sciencedirect.com
SCIENCE DIRECT
Journal of Power Sources 158 (2006) 600–607
JOURNAL OF POWER SOURCES
www.elsevier.com/locate/jpowsour

Effect of an additive to polysiloxane-based electrolyte on passive film formation on a graphite electrode

Hiroshi Nakahara [a,*], Sang-Young Yoon [a], Steven Nutt [b]

[a] *Quallion LLC, Sylmar Biomedical Park, 12744 San Fernando Road, Sylmar, CA 91342, USA*
[b] *Department of Material Science and Engineering, University of Southern California, Los Angeles, CA 90089-0241, USA*

Received 12 September 2005; received in revised form 23 September 2005; accepted 26 September 2005
Available online 14 November 2005

Abstract

Electrochemical impedance spectroscopy (EIS) was performed during the first charge of a graphite/lithium metal test cell to determine the effect of an additive to a polysiloxane-based (PS-B) electrolyte on passive film formation on graphite surface. The graphite electrode was separated from the lithium metal electrode by a porous polyethylene membrane immersed in the PS-B electrolyte containing dissolved vinyl ethylene carbonate (VEC) and lithium bis(oxalato) borate (LiBOB). The presence of the VEC additive suppressed the formation of a gel-like passive film on the graphite electrode, and increased the discharge capacity [H. Nakahara, A. Masias, S.Y. Yoon, T. Koike, K. Takeya, Proceedings of the 41st Power Sources Conference, Philadelphia, 14–17 June, 2004, p. 165]. EIS analysis of the charged graphite electrode revealed that the addition of VEC decreased the passive film resistance, the film capacitance, and the charge transfer resistance. The dependence of film resistance on cell voltage corresponded only to island-like film formation, as opposed to gel-like film formation. This finding was supported by SEM observations that revealed no gel-like film formation [H. Nakahara, A. Masias, S.Y. Yoon, T. Koike, K. Takeya, Proceedings of the 41st Power Sources Conference, Philadelphia, 14–17 June, 2004, p. 165]. The VEC addition decreased the film resistance and the charge transfer resistance, which increased the discharge capacity of the graphite electrode.

Keywords: Lithium battery; Graphite; Siloxane; Additive; LiBOB; Passive film

1. Introduction

Past research has focused on the formation of the solid electrolyte interface (SEI) on the graphite electrode surface in non-aqueous electrolytes, such as the ethylene carbonate/diethyl carbonate system [2,3]. In these reports, the authors determined that exfoliation of graphene layers occurred during initial charging in propylene carbonate-based electrolytes because of co-intercalation of solvent [2,4]. Earlier studies asserted that the SEI film formed mainly by a solvent decomposition reaction, and that it was composed of $ROCO_2Li$ species, Li_2CO_3, and LiF [5–8]. Investigators concluded that the novel lithium salt, lithium bis(oxalato) borate (LiBOB), forms an SEI film directly on graphite, rather than by a solvent decomposition reaction [9–11].

More recent studies have concluded that polysiloxane may be a suitable electrolyte in a lithium polymer battery system because of the high conductivity relative to other polymer materials [12–15]. For example, polyethylene oxide (PEO) is a well-known solid polymer electrolyte that shows conductivity in the range of 10^{-6} to 10^{-7} S cm^{-1} [16]. However, the conductivity of the polysiloxane-based (PS-B) electrolyte exceeds that of PEO by several orders of magnitude, with a value of approximately 10^{-3} S cm^{-1} [17].

The PS-B electrolyte has emerged as a primary candidate for the development of large lithium batteries for applications, such as electric vehicles, in which safety is a prime consideration [17]. Despite numerous reports of SEI film formation in conventional electrolyte, there have been few studies of the SEI formation in PS-B electrolytes. In one report, the existence of two types of passive film and the associated morphological features was revealed by SEM observations [1]. One passive film was island-like and formed directly on the graphite surface, while the other was a gel-like film covering the island-like film [1].

DOI of original article:10.1016/j.jpowsour.2005.09.041.
* Corresponding author. Tel.: +1 818 833 2000; fax: +1 818 833 2001.
E-mail address: hiroshi@quallion.com (H. Nakahara).

0378-7753/$ – see front matter © 2005 Elsevier B.V. All rights reserved.
doi:10.1016/j.jpowsour.2005.09.050

Electrolyte additives have been developed to modify graphite electrode surfaces in order to improve two major performance metrics of the electrode in lithium secondary batteries. The first aim is to reduce the irreversible capacity via additives, such as ethylene sulfide, vinylene carbonate, halogenated solvents, and chloroethylene carbonate [18–23]. The second aim is to increase capacity retention after cycling via additives, such as vinyl acetate, divinyl adipate, and ally methyl carbonate [24–26]. In a recent study, the addition of vinyl ethylene carbonate (VEC) to a PS-B electrolyte increased the discharge capacity of the graphite electrode and inhibited gel-like film formation [1]. However, the reason for the increase in discharge capacity has not been clarified yet.

In a recent study, electrochemical impedance spectroscopy (EIS) was used to analyze changes in the graphite electrode during the initial charging in PS-B electrolytes [27]. The EIS results indicated that the charge transfer resistance was larger than that of the other electrolyte systems. The analysis suggested that decreasing charge transfer resistance was essential to increase the discharge capacity of the negative electrode.

In this study, EIS measurements were performed while charging the graphite electrode with polysiloxane-based electrolyte containing VEC and dissolved LiBOB salt. The objective was to gain understanding of the effect of VEC addition to the PS-B electrolyte on the electrical properties of the graphite surface. The dependences of the resistance and capacitance of the passive films, the electric double-layer capacitance, and the charge transfer resistance on the cell voltage were determined. The findings clarify the underlying causes of the increase in the discharge capacity of graphite electrode after VEC addition to the polysiloxane-based electrolyte, as demonstrated previously [1].

2. Experimental

2.1. Electrode morphology and composition

The molecular structure of poly(dimethyl) siloxane poly(ethylene oxide) investigated in this study is shown in Fig. 1. In the present experiments, the molecule indexed at $m=0$, $n=8$, and $x=3$ was used. Lithium bis(oxalato) borate (Chemetall GmbH), was dissolved in poly(dimethyl) siloxane poly(ethylene oxide) to achieve a 0.8 M concentration for testing. VEC (Sigma–Aldrich) was mixed with the prescribed polysiloxane-based electrolyte as 10 wt%. The electrolyte was a liquid at room temperature.

A PS-B electrolyte containing VEC additive and dissolved LiBOB was used to modify the surface of highly oriented pyrolytic graphite (HOPG). The PS-B electrolyte without VEC was also evaluated as control electrolyte. A block of HOPG

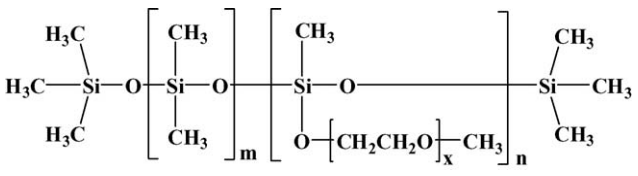

Fig. 1. Molecular structure of poly(dimethyl) siloxane poly(ethylene oxide).

(2 mm × 2 mm × 1 mm) was used as the working electrode. Copper mesh was wrapped around the HOPG block electrode used as a current collector. The electrode was covered with a polyethylene porous separator, and lithium metal was pressed against a copper mesh and used as the counter electrode. The working electrode, counter electrode, separator, and electrolyte were packaged in a heat-sealed aluminum laminated bag. The laminated cell was charged to 0.02 V. The charged electrode was removed from the disassembled cell in a glove box filled with Ar gas, maintaining the dew-point below −75 °C, rinsed with diethyl carbonate (DEC), and dried under vacuum at room temperature. The surfaces of the HOPG were observed by SEM (JEOL JSM-5910LV) after sputter-coating with gold. In addition, the composition of specimens was analyzed using energy dispersive X-ray spectroscopy (EDX; Oxford Instruments, EDS INCAEnergy 7274).

2.2. Electrochemical impedance spectroscopy

The graphite electrodes were prepared by mixing 33.6 g of mesocarbon microbeads (Osaka Gas Co., Ltd., MCMB 25–28), 14.4 g of graphite fiber (Petoca Co., Ltd., GMCF), 62.6 g of 2 wt% aqueous solution of carboxymethyl cellulose (Dai-ichi Kogyo Seiyaku Co., Ltd., Celogen WSC), and 1.88 g of a 40% aqueous dispersion of styrene butadiene rubber (Dai-ichi Kogyo Seiyaku Co., Ltd., BM-400) in a mixer. The mixture was spread on a copper foil (10 μm thick) with a doctor blade and dried in an oven at 80 °C. The dried electrode plate was then pressed using a roll press to a thickness of 102 μm. Pressed electrodes were dried in a vacuum oven at 120 °C for 12 h. The carbonaceous electrodes (15 mm in diameter) were punched out of the dried electrode plate. Lithium metal electrodes (16 mm in diameter) were punched from a lithium metal sheet (Honjo metal, 100 μm thick). Coin cells (2032-type) were prepared by stacking a lithium metal electrode, a separator, a carbonaceous electrode, spacer disks made from stainless steel, and a spring in sequence. The separator was a 25 μm-thick polyethylene porous membrane (Tonen Chemical Co., Ltd.). The polysiloxane-based electrolyte containing VEC additive and dissolved LiBOB was filled into the assembled cell. All parts used for the coin cell assembly were dried in a vacuum oven at 60 °C for more than 8 h.

AC impedance measurements were performed with a potentiostat (Solartron, SI1287) and a transfer function analyzer (Solartron, 1255B). The frequency used for the impedance measurements was 2 mHz to 1 MHz, and the signal amplitude was 10 mV. Potential step coulometry was performed with an electrochemical interface (Solartron, SI1287). Impedance spectra were measured after the cell had been charged at a rate of *C*/200 to the prescribed voltage and maintained at that voltage for 24 h. The voltage was then stepped to the next potential, and the procedure was repeated. In this manner, the cell was charged from the initial open circuit voltage (OCV) down to 0.05 V at 25 °C. The counter electrode and the reference electrode were lithium metal.

The impedance data were analyzed using commercial software (Scribner Associates, Inc., Zview™) that included a batch fitting function. The function was used to perform fitting for multiple sets of impedance spectra step-by-step. In this method,

initial values of the parameter were obtained from values fitted in the previous step. These values were obtained for a set of measured impedance spectra, from which a complex plane plot was generated at a higher voltage. Next, the fitted parameters generated in one step were used as initial values to fit the spectra of the next step. These procedures were repeated in successive steps until the values of the fit parameters converged [28]. The conductivity of electrolyte was calculated using the real part of the impedance obtained in the high-frequency region of the complex plane pot.

2.3. $LiCoO_2$/graphite cell assembly and evaluation

A lithium polymer cell comprised of lithium cobalt oxide ($LiCoO_2$) cathode and a graphite anode was assembled in order to investigate the effect of the polysiloxane-based electrolyte containing the VEC additive on magnitude of discharge capacity.

A mixture was prepared consisting of 10 g of $LiCoO_2$ (Seimi Chemical Co., Ltd.), 0.33 g of acetylene black (Denka Singapore Private Limited), 0.78 g of PVdF (Kureha Chemical Industry Co., Ltd.), and *N*-methyl-2-pyrrolidone (Sigma–Aldrich). The mixture was spread on an aluminum foil and dried in an oven at 80 °C. The dried electrode plate was then pressed to a thickness of 92 μm using a roll press. Pressed electrodes were dried in a vacuum oven at 120 °C for 12 h. The $LiCoO_2$ electrodes (14 mm in diameter) were punched out of the dried electrode plate. Graphite anodes and separators were prepared as described above. Four different concentrations of VEC (0, 5, 10, and 15 wt%) in polysiloxane-based electrolyte were mixed, and filled in assembled coin cells.

Charge and discharge cycles were performed by Arbin battery cycler BT2000 (Arbin Instruments). The coin cells were charged at *C*/50 to 4.1 V for 25 h, and then discharged at *C*/50 to 2.7 V at 25 °C.

3. Implementation of equivalent circuit model

Electrochemical impedance spectroscopy is a powerful tool to investigate electrolyte–electrode interface reactions [29–37]. For example, EIS has been used to analyze the electrochemical lithium intercalation reaction into carbonaceous material in the carbonate electrolyte system, and the subsequent formation of a SEI film [38–44].

EIS data for lithium ion cells and lithium metal cells have been reported extensively [30–32,34,45]. In related work, logic diagrams and equivalent circuits (ECs) have been proposed for cells with a graphite/lithium metal configuration [46–51]. In most of these studies, an *R–C* parallel or *R*–CPE parallel circuit was used to describe the presence of a surface film layer on the electrode [46,48–52]. EC expresses the electric property of graphite electrode charged in polysiloxane-based electrolyte (Fig. 2) [27]. Segments include (a) electric connection resistance and the electrolyte bulk resistance corresponding to the resistance at the highest frequencies, followed by (b) an *R–C* parallel circuit describing the SEI layer in the middle frequency region, and finally, (c) an *R–C* parallel circuit for double-layer capacitance and charge transfer reaction, including a Warburg diffusion term in the low-frequency region corresponding to lithium diffusion in the solid state [38,41,42,49,53].

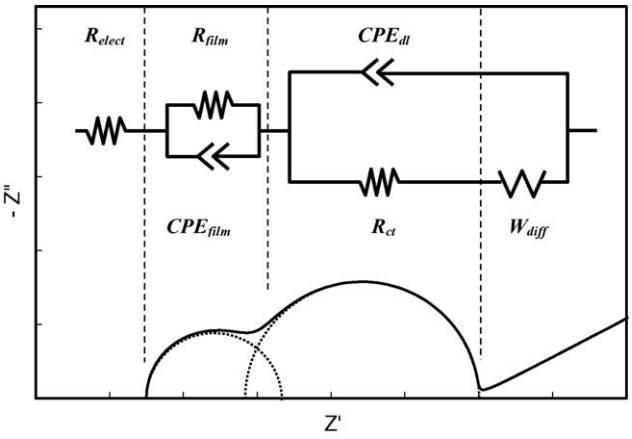

Fig. 2. Equivalent circuit for graphite/polysiloxane-based electrolyte/lithium metal cell.

In general, because semicircles often tend to be depressed in a complex plane plot due to electrode geometry, a constant phase element (CPE) is used in an EC for the porous electrode. The use of a CPE is justified because of the geometrical effect on capacitance in electrochemical reactions [54–56]. The complex impedance of a CPE, Z_{CPE}, is expressed by:

$$Z_{CPE} = \frac{1}{T \cdot (j \cdot \omega)^P} \quad (1)$$

where T represents the pseudo-capacitance that is modified by the electrode geometry, j an imaginary number, and P is an exponential parameter that expresses the electrode geometry as a number. Finally, $\omega = 2\pi f$ is the angular frequency and f is the frequency of the applied AC signal.

In Fig. 2, the EC has the resistance element, R_{elect}, representing the resistance of the bulk electrolyte, and an *R*–CPE parallel circuit [46–51,57–60] for the passive film with resistance R_{film} and constant phase element, CPE_{film}. The final component is an *R*–CPE parallel [61] element that represents the electric double-layer capacitance as a constant-phase element, CPE_{dl}, and the charge transfer resistance, R_{ct}, representing the site where the electrochemical reaction occurs. Each CPE contains the pseudo-capacitance and exponential parameter, as expressed in Eq. (1), i.e., T_{film} and P_{film} for CPE_{film}, and T_{dl} and P_{dl} for CPE_{dl}, respectively. The diffusion impedance $W_{s,diff}$ is connected in series to R_{ct} [55,60,62–64]. For the EC element representing the lithium movement in passive films and the electrochemical reaction at the junction of graphite and electrolyte, a CPE was used in a parallel circuit coupled with a resistance to describe these geometrical features mathematically.

4. Results

4.1. SEM images and EDX qualitative analysis

SEM images of pristine HOPG before lithium intercalation show the smooth surface on the basal plane and the layered appearance on the edge plane (Fig. 3a and b). In addition, the

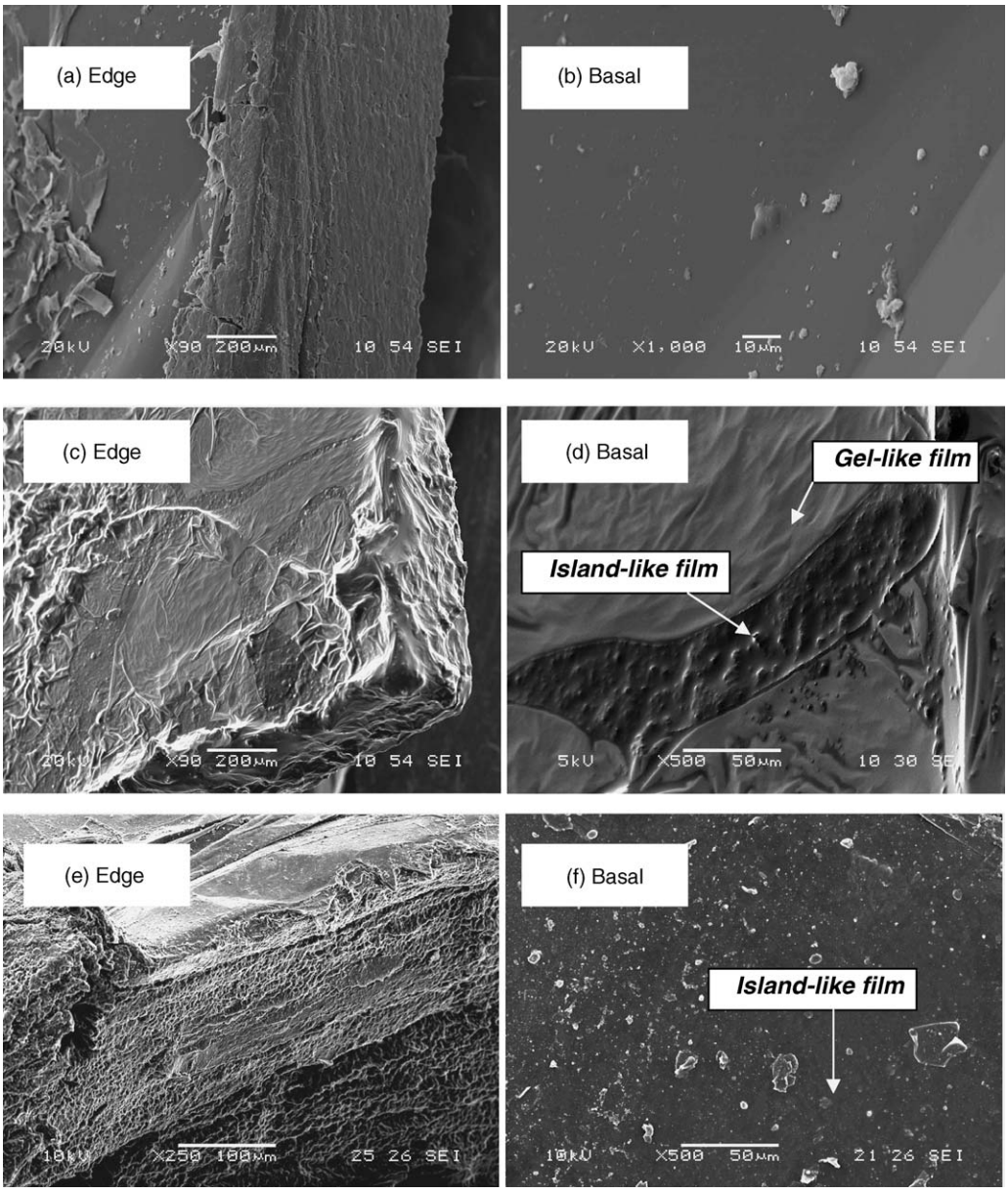

Fig. 3. SEM images of HOPG block charged at 0.02 V vs. Li/Li$^+$: (a and b) before charging, (c and d) after charging in polysiloxane-based electrolyte without VEC (taken from Ref. [2]), and (e and f) after charging in polysiloxane-based electrolyte with VEC.

SEM image of HOPG charged in the PB-S electrolyte excluding VEC is shown in Fig. 3c and d [1]. An island-like film and a gel-like film are apparent on the surface. Furthermore, SEM images of HOPG charged in the PB-S electrolyte with VEC are shown in Fig. 3e and f [1]. There is a significant difference in surface appearance for electrolytes with and without VEC. In the presence of VEC, an island-like film is present on the surface of HOPG, but a gel-like film is not. At last, EDX analyses of the HOPG surface showed the presence of silicon for HOPG charged in the PS-B electrolyte without VEC, although no silicon was present in VEC [1].

4.2. EIS results

The EIS data plots measured at 2.5, 1.7, 0.4 and 0.05 V are shown in Fig. 4. Fig. 4a shows the complex plane plots for PB-S electrolyte without VEC, and Fig. 4b is for that with VEC. The semicircles in the complex plane plots are suppressed and contain more than one semicircle. The semicircle in the middle- or low-frequency region became significantly broader as the cell voltage was decreased. VEC addition decreased the diameter of the semicircle. As the applied voltage was decreased, the straight line in the low-frequency region disappeared, and an additional semicircle was detected.

Fig. 5 shows Bode plots corresponding to the complex plane plots in Fig. 4b. The upper figure (Fig. 5a) shows the logarithm of the measured impedance modulus, $|Z|$, plotted against the logarithm of the applied frequency. The impedance modulus increased with decreasing cell voltage in the frequency range from 0.1 Hz to 1 MHz. The lower figure (Fig. 5b) shows the phase angle of the measured impedance plotted against the applied frequency. While phase angle decreased with lower cell

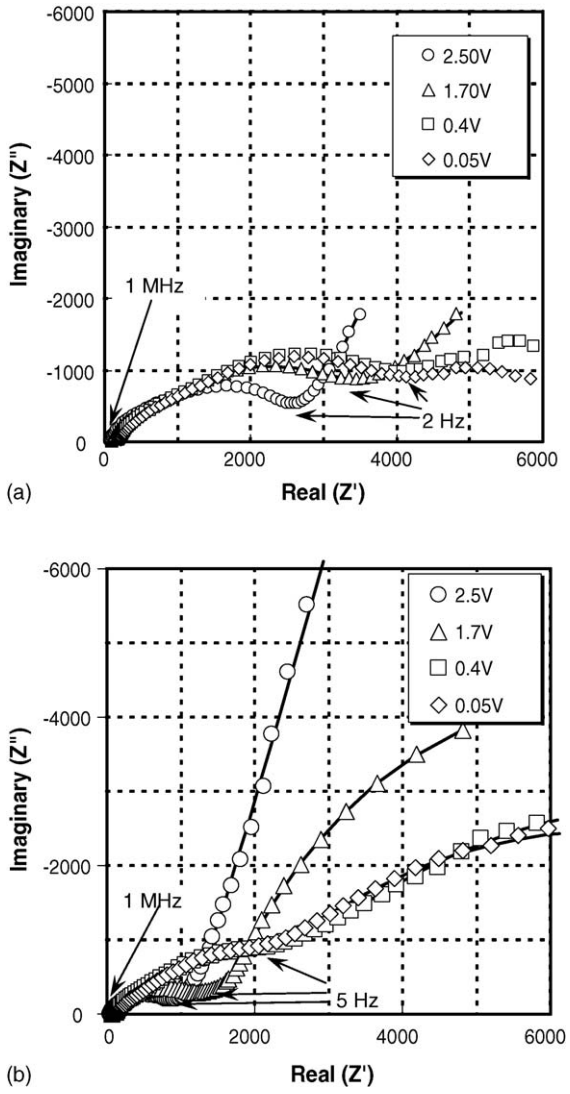

Fig. 4. Nyquist plots for graphite/polysiloxane-based electrolyte/lithium metal cell measured at 2.5, 1.7, 0.4, and 0.05 V vs. Li/Li$^+$: (a) without VEC and (b) with VEC.

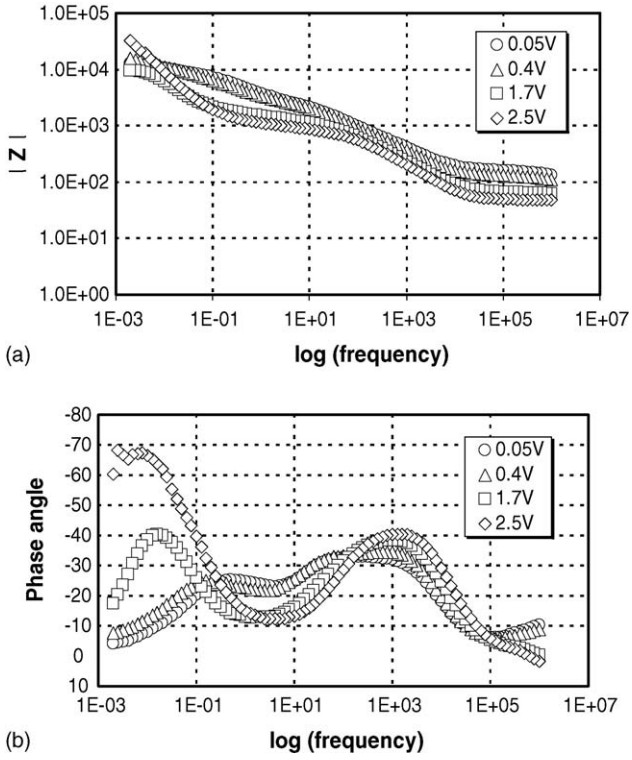

Fig. 5. Bode plots for graphite/polysiloxane-based electrolyte/lithium metal cell measured at 2.5, 1.7, 0.4, and 0.05 V vs. Li/Li$^+$.

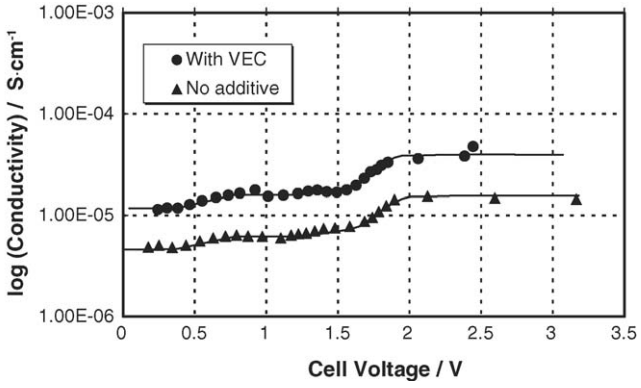

Fig. 6. The calculated conductivity of the electrolyte as a function of the cell voltage.

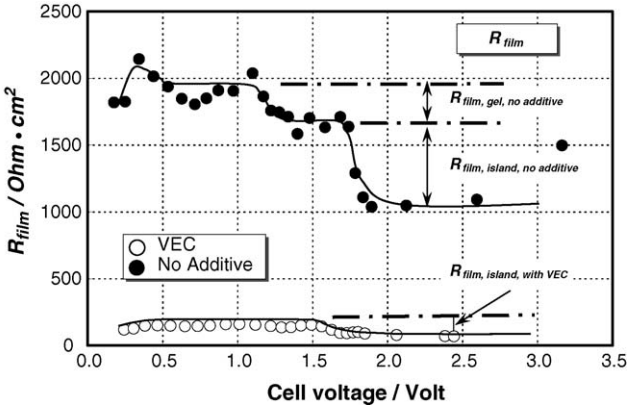

Fig. 7. Values of R_{film} as a function of the voltage of the graphite/polysiloxane-based electrolyte/lithium metal cell.

voltage in the frequency range from 2 to 100 mHz, the phase angle *increased* with lower cell voltage between 10 and 50 Hz.

All impedance elements of the EC depend on the cell voltage. This is illustrated in Fig. 6, where conductivity is plotted versus voltage that was derived using the experimental value of R_{elect}. The addition of VEC increased the electrolyte conductivity over the entire voltage range. Although the electrolyte conductivity both with and without the VEC additive did not change significantly between 2.1 and 3.2 V, the electrolyte conductivity decreased sharply with decreasing cell voltage between 1.6 and 1.9 V, and then more gradually in the ranges of 1.05–1.2 and 0.3–0.5 V. The data indicate that the magnitude of electrolyte conductivity depends on the presence or absence of VEC, although the relative dependencies of electrolyte conductivity on cell voltage for both cases were the same.

The circuit parameters corresponding to the passive films were evaluated to clarify the dependence on cell-voltage. The dependence of R_{film} on cell voltage is shown in Fig. 7, and the

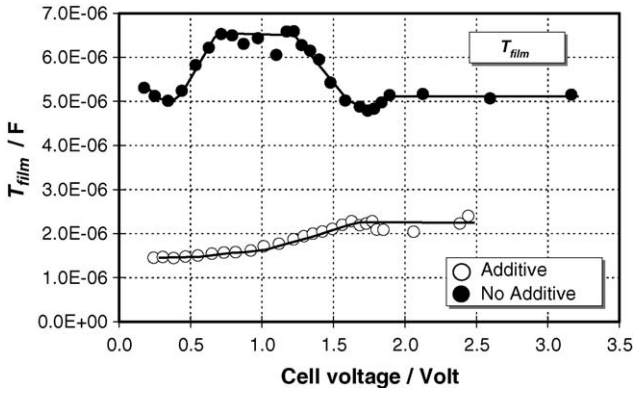

Fig. 8. Values of T_{film} as a function of the voltage of graphite/polysiloxane-based electrolyte/lithium metal cell.

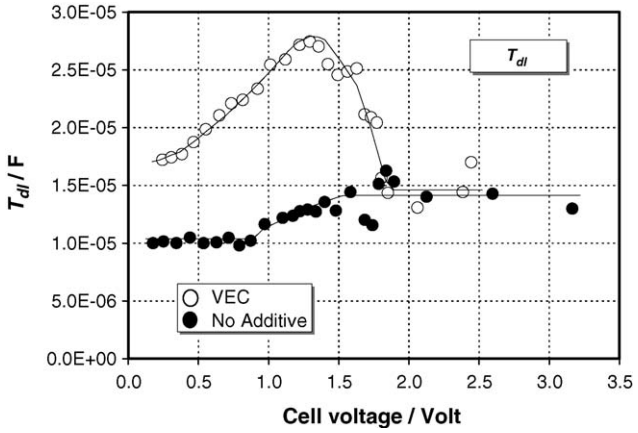

Fig. 9. Values of T_{dl} as a function of the voltage of graphite/polysiloxane-based electrolyte/lithium metal cell.

dependence of T_{film} on cell voltage is shown in Fig. 8. The R_{film} value was constant at voltages above 1.8 V for both electrolytes (with and without VEC), and increased between 1.5 and 1.8 V. While R_{film} for the electrolyte without VEC increased in the voltage ranges of 1.2–1.3 and 0.3–0.5 V, R_{film} for electrolyte with VEC did not change in the voltage range of 0.5–1.5 V. R_{film} for both electrolytes decreased below 0.5 V. While the T_{film} values for electrolyte without VEC rose in the voltage range of 1.2–1.7 V and fell at 0.4–0.6 V (Fig. 8), the T_{film} for electrolyte with VEC showed a constant value in the range above 1.7 V, followed by a monotonic decrease below 1.7 V.

The dependences of the double-layer capacitance parameter on cell voltage, T_{dl}, for electrolyte with and without VEC are shown in Fig. 9. Although the value of T_{dl} for the modified electrolyte did not change above 1.75 V, it increased with decreasing cell voltage between 1.4 and 1.75 V, and decreased monotonically below 1.4 V.

The dependence of the charge transfer resistance, R_{ct}, on the cell voltage is shown in Fig. 10. The value of R_{ct} for both electrolytes was constant above 1.9 V, and increased with decreasing cell voltage below 1.9 V. In contrast, R_{ct} for the modified electrolyte with VEC did not increase between 0.5 and 1.5 V. On the other hand, R_{ct} for the unmodified electrolyte (without VEC) continued to increase between 0.4 and 1.5 V.

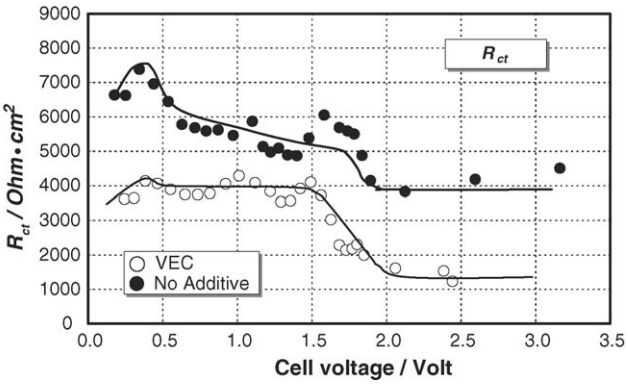

Fig. 10. Values of R_{ct} as a function of the voltage of graphite/polysiloxane-based electrolyte/lithium metal cell.

5. Discussion

The complex plane plots shown in Fig. 4 indicate that the curve calculated using the fit parameters from the proposed EC accurately matches the experimental data (shown with markers). The small uncertainty, χ^2, of the fitting supports the assertion that the proposed EC (Fig. 2) is suitable for modeling the electrochemical reactions in the graphite/polysiloxane-based electrolyte/lithium metal cell system, both with and without VEC. The EC thus constitutes a reliable analog representing the electrochemical properties of the passive films and the electrochemical reaction on the graphite surface.

In earlier work, EIS analysis was shown to correspond to morphological and compositional changes in the surface of HOPG lithiated in PS-B electrolyte without VEC [1,27]. That work led to the conclusion that the increase in passive film resistance, R_{film} at 1.6–1.9 V ($R_{film,\,island,\,no\,additive}$ in Fig. 7) corresponded to formation of an island-like film caused by decomposition of a bis(oxalato) anion [27]. Furthermore, the increase in R_{film} at 1.2–1.4 V ($R_{film,\,gel,\,no\,additive}$ in Fig. 7) was attributed to gel-like film formation initiated by the formation reaction of island-like film [27]. In the present work, no additional increment in R_{film} was observed in the range of 1.2–1.4 V in the presence of VEC. This supports previous assertions about the relationship between the two types of passive film and the increase in R_{film}.

The morphological and electrochemical roles of the VEC additive were manifest in a variety of experimental data and observations. SEM inspection showed the absence of a gel-like film on the HOPG after charged in the VEC-modified electrolyte. These observations were consonant with EIS, and suggest that VEC prevents the formation of a gel-like film over the island-like film, and that the gel-like film was composed of a polysiloxane derivative [1]. In the presence of the VEC additive, the increment in R_{film} in the range of 1.6–1.9 V ($R_{film,\,island,\,with\,VEC}$) was only 92 Ω cm^2, in contrast with the 670 Ω cm^2 measured in no additive electrolyte ($R_{film,\,island,\,no\,additive}$). In addition, the film capacitance, T_{film} decreased monotonically below 1.9 V in the presence of VEC (Fig. 8). These results indicate that the VEC addition altered the nature of the passive film, which became thinner and/or smoother [27,49].

Earlier work showed that the gel-like film was formed from by-products generated by decomposition of polysiloxane molecules and the bis(oxalato) borate anion [27]. Based on SEM observations, EDX analysis, and the dependence of R_{film} on cell voltage, the VEC molecule appears to scavenge the active species, causing the gel-like film produced by decomposition of the bis(oxalato) borate anion. Furthermore, although no other passive films were detected, this does not preclude the possibility of a passive film arising from a completely different source, such as a VEC reaction with an active decomposed anion. The detailed electrochemical mechanism of formation or prevention of the gel-like film awaits further investigation.

Changes in the conductivity for the VEC-modified electrolyte showed tendencies similar to the standard electrolyte. Earlier work concluded that the observed conductivity change derived from the change in electric contact resistance among graphite particles associated with the formation of passive films [27]. In the present work, the decrease in conductivity with or without VEC exhibited the same magnitude and dependence on cell voltage. Consequently, the decrease in electrolyte conductivity was related to formation of the island-like film, not the gel-like film. The relative contributions of these factors are presently under investigation.

The dependence of both R_{ct} and T_{dl} on cell voltage was simpler for the VEC-modified electrolyte than for the standard electrolyte, apparently because of VEC-induced modifications to electrochemical reactions on the graphite electrode surface. The increase in T_{dl} at 1.3–2.0 V arises from the increase in surface area caused by island-like film formation. Likewise, the decrease in T_{dl} below 1.3 V corresponds to the formation of a smoother surface caused by coalescence within the island-like film. The increase in R_{ct} in the range of 1.5–2.0 V indicates that the growth of the island-like film inhibited the charge transfer reaction on the graphite surface. Furthermore, this increased the surface contact area available for electrochemical reaction between the graphite surface and the electrolyte. No change was observed in R_{ct} for the VEC-modified electrolyte in the range of 0.5–1.5 V, indicating that sites at the boundary between graphite surface and island-like film were unchanged.

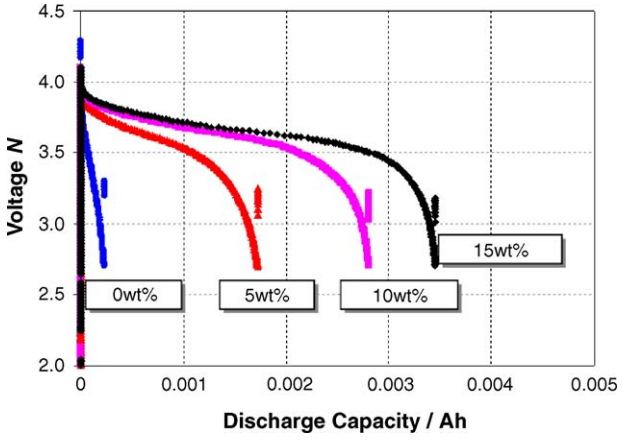

Fig. 11. Discharge curves of $LiCoO_2$/graphite coin cells with polysiloxane-based electrolyte added with different amounts of VEC (taken from Ref. [1]).

The magnitude of R_{ct} for the VEC-modified electrolyte was 1325–4241 $\Omega\,cm^2$, a substantial decrease compared to the magnitude of 3797–7418 $\Omega\,cm^2$ for the standard electrolyte [27]. However, this value was greater than values for the carbonate solvent dissolving $LiPF_6$ (3–10 $\Omega\,cm^2$ [40]), and for the carbonate solvent dissolving $LiCiO_4$ (60–80 $\Omega\,cm^2$ [44]). The electric double-layer capacitance, T_{dl}, fell in the same range of values observed in other studies [27,27].

The discharge capacity of the $LiCoO_2$/graphite cell increased because of VEC addition, as shown in Fig. 11 [1]. The increase in discharge capacity was associated with decreases in film resistance and charge transfer resistance. In addition, the increase in electrolyte conductivity contributed to the observed increase in discharge capacity.

6. Conclusions

Characteristics of the island-like film on a graphite electrode were altered by VEC addition. In particular, charge transfer resistance and passive film resistance were decreased. The enhanced electrical properties of the graphite electrode in the presence of VEC produced an increase in the discharge capacity of the electrode.

Modifying the nature of the passive film significantly affected the electrochemical performance of a graphite electrode. The VEC addition modified passive films on the HOPG surface morphologically and compositionally. The VEC additive effectively prevented the formation of the gel-like film produced by cross-linking polysiloxane molecules. Furthermore, EIS analysis revealed that the electrical characteristics of the electrodes, such as high-current discharge capability, presently prevent the commercial use of polysiloxane-based electrolytes [65].

The charge transfer resistance for the present electrolyte system was still greater than that of conventional carbonate electrolyte systems. Clearly, further reduction in the charge transfer resistance is required to realize the commercialization of polysiloxane-based electrolyte. To achieve this reduction, the types of salt and polysiloxane molecular structures reported here, while viable candidates for a battery system will require optimization of the salt and polysiloxane molecular structure through surface modification. Microscopic observations and EIS analysis should provide further insights into the nature and formation mechanisms of passive films, and expedite optimization.

Acknowledgements

The support for this study from the US Army Communications-Electronics Command Center (CECOM), University of Wisconsin, and Argonne National Laboratory is gratefully acknowledged. Helpful suggestions from Prof. F. Mansfeld are also gratefully acknowledged.

References

[1] H. Nakahara, A. Masias, S.Y. Yoon, T. Koike, K. Takeya, Proceedings of the 41st Power Sources Conference, Philadelphia, 14–17 June, 2004, p. 165.

[2] M. Inaba, Z. Shiroya, Y. Kawatate, A. Funabiki, Z. Ogumi, J. Power Sources 68 (2) (1997) 221–226.
[3] S.-K. Jeong, M. Inaba, Y. Iriyama, T. Abe, Z. Ogumi, Electrochim. Acta 47 (2002) 1975–1982.
[4] R. Mogi, M. Inaba, Y. Iriyama, T. Abe, Z. Ogumi, J. Power Sources 108 (2002) 163–173.
[5] D. Aurbach, E. Zinigrad, Y. Cohen, H. Teller, Solid State Ionics 148 (2002) 405–416.
[6] D. Aurbach, I. Weissman, A. Zaban, P. Dan, Electrochim. Acta 45 (1999) 1135–1140.
[7] D. Aurbach, A. Zaban, Y. Gofer, Y.E. Ely, I. Weissman, O. Chusid, O. Abramson, J. Power Sources 54 (1995) 76–84.
[8] Z. Ogumi, A. Sano, M. Inaba, T. Abe, J. Power Sources 97–98 (2001) 156–158.
[9] K. Xu, S. Zhang, B.A. Poese, T.R. Jow, Electrochem. Solid-State Lett. 5 (1) (2002) A259–A262.
[10] K. Xu, S. Zhang, T.R. Jow, W. Xu, C.A. Angell, Electrochem. Solid-State Lett. 5 (1) (2002) A26–A29.
[11] K. Xu, S. Zhang, T.R. Jow, Electrochem. Solid-State Lett. 6 (6) (2003) A117–A120.
[12] Y. Kang, W. Lee, D.H. Suh, C. Lee, J. Power Sources 119–121 (2003) 448–453.
[13] I.J. Lee, G.S. Song, W.S. Lee, C. Lee, J. Power Sources 114 (2003) 320–329.
[14] M. Shibata, T. Kobayashi, R. Yosomiya, M. Seki, Eur. Polym. J. 36 (2000) 485–490.
[15] Z. Zhang, S. Fang, Electrochim. Acta 45 (2000) 2131–2138.
[16] Z. Wang, M. Ikeda, N. Hirata, M. Kubo, T. Ito, O. Yamamoto, J. Electrochem. Soc. 146 (6) (1999) 2209–2215.
[17] B. Oh, D. Vissers, Z. Zhang, R. West, H. Tsukamoto, K. Amine, J. Power Sources 119–121 (2003) 442–447.
[18] M.-S. Wu, P.-C.J. Chiang, J.-C. Lin, J.-T. Lee, Electrochim. Acta 49 (2004) 4379.
[19] G.H. Wrodnigg, J.O. Besenhard, M. Winter, J. Eletrochem. Soc. 146 (1999) 470.
[20] Y. Naruse, S.Fujita, A. Omaru, US Patent 5,714,281 (1998).
[21] D. Aurbach, K. Gamolsky, B. Markovsky, Y. Gofer, M. Schmidt, U. Heider, Electrochim. Acta 47 (2002) 1423.
[22] Z.X. Shu, R.S. McMillan, J.J. Murrary, J. Electrochem. Soc. 142 (1995) L161.
[23] Z.X. Shu, R.S. McMillan, J.J. Murrary, I.J. Davidson, J. Electrochem. Soc. 143 (1996) 2230.
[24] K. Abe, H. Yoshitake, T. Kitakura, T. Hattori, H. Wang, M. Yoshio, Electrochim. Acta 49 (2002) 4613.
[25] C. Wang, H. Nakamura, H. Komatsu, M. Yoshio, H. Yoshitake, J. Power Sources 74 (1998) 142.
[26] H. Yoshitake, K. Abe, T. Kitakura, J.B. Gong, Y.S. Lee, H. Nakamura, M. Yoshio, Chem. Lett. 32 (2003) 134.
[27] H. Nakahara, S.Y. Yoon, T. Piao, S. Nutt, F. Mansfeld, J. Power Sources 158 (2006) 591–599.
[28] C.S. Wang, A.J. Appleby, F.E. Little, Electrochim. Acta 46 (2001) 1793.
[29] N. Hiroyoshi, S. Kuroiwa, H. Miki, M. Tsunekawa, T. Hirajima, Hydrometallurgy 74 (2004) 193.
[30] K. Abe, H. Yoshitake, T. Kitakura, T. Hattori, H. Wang, M. Yoshio, Electrochim. Acta 49 (26) (2004) 4613.
[31] M.-S. Wu, P.-C.J. Chiang, J.-C. Lin, J.-T. Lee, Electrochim. Acta 49 (2004) 4379.
[32] M.S. Michael, S.R.S. Prabaharan, J. Power Sources 136 (2004) 250.
[33] S.-H. Choi, J. Kim, Y.-S. Yoon, Electrochim. Acta 50 (2–3) (2004) 547.
[34] C.H. Chen, J. Liu, M.E. Stoll, G. Henriksen, D.R. Vissers, K. Amine, J. Power Sources 128 (2004) 278.
[35] J.-H. Kim, C.W. Park, Y.-K. Sun, Solid State Ionics 164 (2003) 43.
[36] Z.P. Guo, S. Zhong, G.X. Wang, H.K. Liu, S.X. Dou, J. Alloys Compd. 348 (2003) 231.
[37] S.S. Zhang, T.R. Jow, J. Power Sources 109 (2002) 458.
[38] S. Zhang, P. Shi, Electrochim. Acta 49 (2004) 1475.
[39] Z. Ogumi, T. Abe, T. Fukutsuka, S. Yamate, Y. Iriyama, J. Power Sources 127 (2004) 72.
[40] S. Komaba, T. Itabashi, B. Kaplan, H. Groult, N. Kumagai, Electrochem. Commun. 5 (2003) 962.
[41] J. Yao, G.X. Wang, J.-H. Ahn, H.K. Liu, S.X. Dou, J. Power Sources 114 (2004) 292.
[42] M. Nookala, B. Kumar, S. Rodrigues, J. Power Sources 111 (2002) 165.
[43] Y.-K. Choi, K.-I. Chung, W.-S. Kim, Y.-E. Sung, S.-M. Park, J. Power Sources 104 (2002) 132.
[44] S.B. Lee, S.-I. Pyun, Carbon 40 (2002) 2333.
[45] B. Jin, J.-U. Kim, H.-B. Gu, J. Power Sources 117 (2003) 148.
[46] C.R. Yang, J.Y. Song, Y.Y. Wang, C.C. Wan, J. Appl. Electrochem. 30 (2000) 29.
[47] Y.C. Chang, J.H. Jong, G.T.K. Fey, J. Electrochem. Soc. 147 (2000) 2033.
[48] Y.C. Chang, H.J. Sohn, J. Electrochem. Soc. 147 (2000) 50.
[49] M. Holzapfel, A. Martinent, F. Alloin, B. Le Gorrec, R. Yazami, C. Montella, J. Electroanal. Chem. 546 (2003) 41.
[50] T. Piao, S.M. Park, C.H. Doh, S.I. Moon, J. Electrochem. Soc. 146 (1999) 2794.
[51] F. Prieto, I. Navarro, M. Rueda, J. Electroanal. Chem. 550–551 (2003) 253.
[52] N. Hiroyoshi, S. Kuroiwa, H. Miki, M. Tsunekawa, T. Hirajima, Hydrometallurgy 74 (2004) 193.
[53] S. Yoon, H. Kim, S.-M. Oh, J. Power Sources 94 (2001) 68.
[54] J.R. MacDonald (Ed.), Impedance Spectroscopy: Emphasizing Solid Materials and Systems, John Wiley & Sons, New York, 1987.
[55] J. Bisquert, A. Compte, J. Electroanal. Chem. 499 (2001) 112.
[56] Y.O. Kim, S.M. Park, J. Electrochem. Soc. 148 (2001) A194.
[57] E. Basrsoukov, J.H. Kim, C.H. Yoon, H. Lee, J. Electrochem. Soc. 145 (1998) 2711.
[58] J.-S. Kim, Y.-T. Park, J. Power Sources 91 (2000) 172.
[59] M.W. Wagner, Electrochim. Acta 10 (1997) 1623.
[60] V. Doge, J. Dreher, G. Hambitzer, IEEE 0-7803-2459-5/95, 1995.
[61] S. Buller, M. Thele, R.W. De Doncker, IEEE 0-7803-0/03, 2003.
[62] I. Uchida, M. Mohamedi, K. Dokko, M. Nishizawa, T. Itoh, M. Umeda, J. Power Sources 97–98 (518) (2001).
[63] R.M. Spotnitz, IEEE 0-7803-5924-0/00, 2000.
[64] M.J. Issacson, N.A. Torigoe, R.P. Hollandsworth, IEEE 0-7803-4098-1/98, 1998.
[65] S.-Y. Yoon, H. Nakahara, Z. Zhang, Q. Wang, K. Amine, R. West, H. Tsukamoto, Proceedings of the Second International Conference on Polymer Batteries and Fuel cells, Las Vegas, USA, 12–17 June, 2005 (Abstract No. 121).